LEVEL

ONR TECHNICAL REPORT
JWTR-5
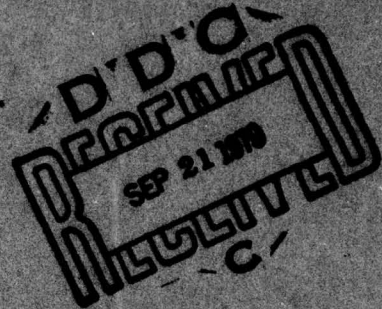
SEP 21 1979

"Phase Transformations and Tensile
Properties of Ti-10V-2Fe-3Al"

Department of Metallurgy and Materials Science

Carnegie-Mellon University

Pittsburgh, PA 15213

August, 1979

PHASE TRANSFORMATIONS AND TENSILE PROPERTIES OF Ti-10V-2Fe-3Al

T. W. Duerig,[*] G. T. Terlinde[*] and J. C. Williams[*]

[*]Department of Metallurgy and Materials Science,
Carnegie-Mellon University, Pittsburgh, PA 15213

INTRODUCTION

Demands for high strength light-weight alloys have been steadily increasing in recent years. Although the well established α and $\alpha+\beta$ titanium alloys (such as Ti-6Al-4V) have successfully met many of these demands, they are unsuited for thick section applications due to their extremely rapid decomposition kinetics. This has shifted research interests to the β Ti alloys, so called because the high temperature BCC phase (β) is chemically stabilized and can be retained upon quenching. When compared to the α and $\alpha+\beta$ alloys, β alloys enjoy the advantages of increased strength-to-density ratios, improved formabilities, lower thermal processing costs, and most importantly, improved deep hardenabilities.

Ti-10V-2Fe-3Al is a relatively new β Ti alloy, in which the high temperature β-phase is stabilized by nominal alloying additions of 2wt%Fe and 10wt%V. The 3% Al is a natural ingredient in the master alloy and acts as a solid solution strengthener for the low temperature precipitating α-phase (HCP). This partic-ular alloying combination results in a nominal β-transus of $\sim 800^{\circ}$C, which is relatively high when compared to other β alloy systems. Generally the more heavily β-stabilized alloys (such as β-III, Ti-8V-8Mo-2Fe-3Al, etc) suffer from higher densities, higher manufacturing costs, and slower age hardening kinetics than Ti-10V-2Fe-3Al. This paper describes the results of a research program conducted to identify the various phase transformations of Ti-10-2-3, and to relate these to basic tensile properties.

EXPERIMENTAL

The material used in this study originated from Timet heat #P 1452. The specific heat chemistry is:

Element	V	Fe	Al	O	N	C	Ti
concentration (weight percent)	10.3	2.2	3.2	0.15	.009	.016	Bal.

The β-transus was measured as 805±3°C, somewhat high compared to other 10-2-3 heats. This probably reflects the oxygen content which is on the high side of the normal range. The thermo-mechanical processing began with a 7000 pound ingot which was upset forged 35% at 1120°C, drawn to an 18" square, and subsequently forged to a plate of 8" x 2" cross-section. The slab was then cut and hot rolled from 730°C to a 1" x 4-1/2" plate.

All subsequent heat treatments were done in laboratory-type apparatus using small specimens. Treatments above 600°C were done by vacuum encapsulating specimens wrapped with Ta foil. Below 600°C, treatments were performed in a liquid nitrate salt bath.

Metallographic specimens were electropolished in a 5% H_2SO_4 + 1%HF + balance methanol solution at a closed circuit voltage of 21 volts. The primary etchant was prepared with equal parts of 10% oxalic acid and 1%HF in water.

Thin foils for Transmission Electron Microscopy (TEM) were prepared in a Fishione twin jet electropolishing unit with either a 6% percloric + 31% butanol + 63% methanol solution, or a 5%H_2SO_4 + 95% methanol solution chilled to -50°C. The foils were examined in a variety of electron microscopes. Instruments used were a JEOL 100B, JEOL 100C, and JEOL 100CX TEMSCAN equipped with a Kevex Quantex energy dispersive X-ray spectrometer. Scanning Electron Microscopy (SEM) was done on a JSM-35.

Tensile testing was performed on an Instron machine using a clip-on extensometer. The strain rate was .00055 sec^{-1}, and the tensile specimen gage sections were .640cm in diameter and 3.2cm in length.

RESULTS AND DISCUSSION

I. Microstructural

For organizational purposes, the results of the microstructural study of 10-2-3 can be sub-divided into sub-sections. These are listed below along with the content of each sub-section:

- 2 -

A. **Thermomechanically processed and/or annealed microstructures -**

Characterization of the hot rolled material and discussion of the various microstructural changes which occur during solution treating.

B. **Quenching Transformations -**

Discussion of the athermal β to ω transformation.

C. **Isothermal Aging Transformations -**

Description of the isothermal $\beta-\omega$ reaction and three morphologies of α precipitation.

D. **Stress Assisted Transformations -**

Discussion of the martensitic transformation of β to α'' orthorhombic martensite during straining.

Each of these topics will be separately discussed. The effect of these various microstructural modifications on mechanical response will be discussed in a separate section.

Other work[1-3] has shown that minor modifications of thermomechanical processing (TMP) histories influence 10-2-3 microstructures quite strongly. For example:

1. High deformation rates and high temperatures encourage dynamic recrystallization, leading to an equiaxed β grain structure. Low temperatures and deformation rates, on the other hand, result in a highly deformed β grain structure.

2. Volume fraction of primary α (defined as α present at the temperature of TMP completion) can be directly related to TMP temperature.

3. High deformation rates tend to break-up primary α (α_p) particles, and thereby reduce their aspect ratio.

- 3 -

Only one TMP schedule was investigated in this study. Thus, it is appropriate to carefully document the as-rolled microstructure since it represents the starting point for all subsequent microstructural modifications.

A. Thermo-Mechanically Processed and Annealed Structures

Figure 1a shows the microstructure of 10-2-3 as hot rolled by Timet in the aforementioned manner.

Low magnification studies show an inhomogeneous distribution of α_ρ. The elongated regions which contain a lower amount of α_ρ are termed bands. The smallest dimension of the bands is oriented parallel to the short transverse direction of the plate. Figure 1b shows actual denuded bands in an annealed specimen. Analytical microscopy X-ray analysis has shown these bands to be $\sim$ 50% enriched in Fe, and to have the bulk average Al and V content. TEM investigations of the as-rolled structure show that both the β matrix and the α_ρ are polygonized. More detailed examination revealed a small amount of fine α on subgrains, and a uniform dispersion of athermal ω, which will be discussed below.

Solution treating subsequent to TMP can be performed either above the 805°C β-transus (β-ST) or below it (α+β-ST). Examples of both are given in Figure 2. From these it can be seen that no athermal martensite forms on quenching 10-2-3 from above the β-transus. Thus the M_s of the alloy must lie beneath room temperature. Inclusions of a 1μm average diameter are more readily observed in Figure 2a, but are present in all conditions. Figure 3 shows an inclusion in TEM bright field, with associated X-ray spectra of both the matrix and the inclusion. Repeated analysis of these inclusions has shown that the inclusion compositions are somewhat variable but typically fall in the following atomic percent ranges:

Silicon	1.5 - 2.5
Phosphorous	10. - 15.
Sulfur	2. - 5.
Titanium	80. - 83.

- 4 -

Such inclusions (as well as the aforementioned banding) are common not only to 10-2-3, but to most β-Ti alloys, making the results of this paper pertinent to most commercial heats of β-Ti alloys.

Of the various microstructural modifications brought about by solution treating the as-rolled material, the most rapid is the equilibration of α-phase volume fraction. Figure 4 relates equilibrium α to solution treatment (ST) temperature. This data was obtained by a Quantimet 7000, and independently confirmed by manual quantitative metallography. Equilibration is very rapid due to the high diffusivities of both Fe and V. Five minutes at 850°C is sufficient to dissolve all α_ρ in the hot rolled material. Following equilibration, the α_ρ begins to change from the plate morphology preferred during growth to the lower surface area sphere morphology. Subsequent coarsening is very slow. Matrix recrystallization has been observed to be extremely rapid during β-ST treatments, but extremely slow when α_ρ is present. For example, 5 minutes at 850°C completely recrystallizes the β grain structure, but 10^4 minutes at 760°C has very little effect upon the rolled structure. The most important effect of any solution treatment, however, is to control the β-phase stability after subsequent quenching. Clearly, a lower ST temperature will result in a more stable, solute-rich, as-quenched β matrix, and a lower driving force for subsequent decomposition behavior. The importance of this will be shown in the mechanical property discussion.

B. Transformation Products of Quenching

There are two types of athermal transformation products found in Ti alloys: athermal ω (ω_a) and various martensites. Although both can be found in quenched 10-2-3 specimens, the latter is attributable to quenching strains, rather than to the quench itself, and therefore is more appropriately discussed in a later

section where stress assisted transformations are discussed.

The athermal β to ω transformation was shown to occur uniformly throughout the β-phase in all solution treated and quenched material with less than ∿ 30% α_ρ vol by (Figure 5). Although verified to be a diffusionless process by rapid quenching experiments,[4] the athermal β→ω transformation is not martensitic in the classical sense. De Fontaine and others[5,6] have shown that the instability of the β matrix with respect to $\frac{2}{3}$ <111> longitudinal displacement waves could lead to a local ordering of displaced {111} planes, with a resulting structural transformation. The structure formed by such an event is the ω-phase, which has a hexagonal cell (P6/mmm) with c/a = .613 and atoms positioned at (0,0,0), (1/3, 2/3, 1/2), and (2/3, 1/3, 1/2). Further, the orientation relation first suggested by Silcock,[7] and which has been shown in many alloys[8,9] is in keeping with the transformation mechanism just discussed. This relation is:

$$(0001)_\omega \ || \ (111)_\beta$$
$$(11\bar{2}0)_\omega \ || \ (1\bar{1}0)_\beta \ .$$

Energetically, this diffusionless transformation can be understood using the schematic free energy curves of Figure 6. Shown are the equilibrium α and β curves, as well as the metastable ω curve, for the composition range central to this discussion.

With sufficiently high diffusion rates, ω would form at composition A and the matrix composition would change to C. Thus, the most energetically favorable metastable configuration can be achieved without the intervention of α. During and following a quench, diffusion is not rapid enough to allow this. Between compositions A and B, however, the β→ω transformation is energetically favorable without diffusion, and can occur if nucleation is sufficiently easy. De Fontaine's

displacement wave formation process requires no nucleation per se and has little or no activation barrier. Thus, the ω_a is formed immediately upon quenching. At first glance, it may appear that the transformation should go to completion once it has begun, but this need not be true. Since the athermal ω-phase is accompanied by a change in specific volume, it can be locally elastically stabilized or destabilized depending on local defects such as vacancy clusters. During a quench, athermal ω first appears in the vicinity of local defects whose displacement fields favor the ω-β dilation. As the quench continues, and ω continues to form, the ω_a particles will begin to elastically interact. Such an elastic interaction will halt growth and stabilize the $\beta + \omega_a$ matrix against further transformation.

C. Isothermal Aging Products

Although the β stability of solution treated and quenched 10-2-3 is somewhat affected by the athermal formation of ω, there remains a considerable driving force available for diffusional transformations. The response of β-ST and quenched 10-2-3 to isothermal aging has been studied and is separately discussed in two categories—(i) the isothermal continuation of ω, and (ii) the precipitation of α.

i - Isothermal Omega

Before discussing the isothermal $\beta \rightarrow \omega$ reaction, it is appropriate to first discuss how the $\beta + \omega_a$ matrix is altered by rapidly heating to the aging temperature (T_a). If T_a is sufficiently high, ω_a will completely revert to β. Below about 450°C, however, only partial reversion occurs, with a greater number of ω_a particles reverting as T_a approaches 450°C. The particles situated at elastically stabilizing defects will persist to the highest temperatures, and will also be the largest particles present at room temperature.

At temperatures where α nucleation is very sluggish due to slow diffusion rates, the stability of the $\beta+\omega_a$ matrix can still be increased by the short range diffusionally-assisted movement of the $\beta-\omega_a$ interface into the β matrix. To better understand how this is done, it is necessary to again refer to Figure 6. Now assume the curves apply to T_a and that the overall composition falls between B and C. Classical precipitation theory requires local fluctuations in composition sufficient to permit the local matrix composition to become A. However, since the ω-phase is already present and can rapidly expand, and because diffusion is slow, the $\beta-\omega$ interface will advance into the β field before A is achieved. Limited diffusion is still required since composition B must be achieved before ω is energetically preferable to β. Subsequent enrichment of the ω-phase in Ti (depletion of Fe and V) eventually leads to metastable equilibrium where the ω composition is A. This chemical equilibration is completed after the ω volume fraction has stabilized.

At 250°C (Figure 7a) very little athermal ω is reverted during heat-up, and thus a high density of fine isothermal ω (ω_{iso}) is observed. On the other hand, at 400°C (Figure 7b) nearly all the ω_a is reverted, and only the most stable ω_a remain and grow by the displacement-diffusion mode mentioned above.

Earlier studies[8,10,11] have consistently shown that high misfit systems such as Ti-V and Ti-Fe tend to form cuboids of ω in contrast with the ellipsoids found in low misfit systems. The accepted explanation of this difference is that in high misfit systems, strain energy minimization is important, while in low misfit systems surface energies dominate. Since Ti-10V-2Fe-3Al is a high misfit system, one should expect cuboidal ω. Such is not necessarily the case. Prior to the completion of chemical partitioning, the ω has a low misfit. Thus,

- 8 -

ellipsoids should be expected after very short aging times at temperatures where the displacement-diffusion process leads to large particles (Figure 7b). Due to diffusional partitioning of solute during continued aging, the β-phase lattice parameter contracts. As this occurs, the ellipsoidal ω particles are subjected to an increasing and finally a high misfit,and the expected cuboids are observed (Figure 7c). Thus, three ω morphologies are found in 1C-2-3:

1. Non-descript (Figure 7a) - Found at low
   temperatures where particle density
   is very high. This morphology is possibly
   the result of elastic particle interactions.
2. Ellipsoidal (Figure 7b) - Resulting from the
   rapid displacive growth of athermal ω, prior
   to chemical equilibration.
3. Cuboidal (Figure 7c) - Resulting from the high
   misfit ω particles found after chemical
   partitioning.

ii.- Isothermal Alpha

The equilibrium α-phase in Ti-10-2-3 can form by any one of three nucleation schemes. As will be shown, each nucleation regime results in a distinct morphology and distribution of α. The relative activities of these nucleation modes are controlled by the aging temperature.

At relatively low aging temperatures (below ∿ 450°C), the appearance of α is preceded by ω. As has been suggested in other β Ti alloy systems,[8] the ω particles appear to provide preferential nucleation sites for α. Evidence for this is derived from Figure 8a. Here, extremely fine α of non-descript shape is observed uniformly throughout the β matrix. No preference for nucleation at

dislocations or boundaries is observed. The α-phase particle size and distribution closely resembles that of the preceding β+ω structure (Figure 7b). Although the precise precipitation mechanism involved is unclear, it has been suggested[10,11] that as ω particles are aged, their associated lattice misfit is increased. Dislocations may then either migrate to, or form at, the β+ω interface. The resulting discontinuity at the β/ω interface may then provide a preferential site for α nucleation. These α nuclei should then rapidly consume the volume occupied by ω-phase, but then only slowly expand into the surrounding matrix. There are two possible reasons for such a biased growth.

1. Since the ω-phase is rich in Ti, the β-ω interface represents a discontinuity in both composition and structure. Although the ω structure may be more conducive to α formation, it is certain that the ω→α transformation requires less diffusion than the β→ω transformation.

2. There is evidence that when coherency is lost, the ω particles become unstable. This may also promote α formation.

After the ω-phase is consumed by α, the new α particle may begin to grow into the β matrix. During this later stage, uniform distribution of small, closely-spaced plates may result.

In Ti alloys, there are two crystallographic types of α: Burger's α, which follows the orientation relationship

$$(111)_\beta \ || \ (11\bar{2}0)_\alpha$$
$$[110]_\beta \ || \ [0001]_\alpha$$

and non-Burger's α, which follows a complex orientation that is yet to be conclusively identified. Although both types of α are common in 10-2-3, all α precipitated in this low temperature regime is of the first type. Thus, in 10-2-3, Burger's α is observed as a precursor to non-Burger's α. This supports previous work[12] indicating that non-Burger's α is the more stable of the two forms.

Above 400°C, there is sufficient thermal activation to allow a second nucleation scheme. Here the α-phase nucleates nonuniformly as high aspect ratio plates bearing no relationship to the previous $\beta+\omega$ dispersion (Figure 8b). Although a definite preference for grain boundary nucleation is demonstrated, there is also evidence of "sympathetic nucleation" within the grains. The term "sympathetic nucleation" was first coined by Aaronson[13] to describe the ability of extant α plates to enhance subsequent α nucleation. Although elastic stress fields can often be the cause for this accelerated nucleation, in this case it is more likely that either the dislocation network punched out during formation of previous plates or the α-β surface itself is acting to enhance the nucleation rate.

Although this type of nucleation is active over a wide temperature range, the best support for it is found at 400°C, where sympathetic plate nucleation must compete with the uniform process discussed above. In this transition regime, plate nucleation is still somewhat slow due to the limited diffusion. Once a plate is nucleated, however, subsequent sympathetic branching is rapid. Thus, a blotchy or patchy α-phase precipitate distribution is observed (Figure 9). Here the unetched white regions contain the fine uniform precipitation product, while the dark patches are composed of the sympathetic plates. Since the uniform α precipitation process increases β stability uniformly throughout the β matrix, the rate of expansion of the sympathetically nucleated patches slows

with increasing aging time and effectively ceases.

A third precipitation regime is evident at higher temperatures (above 650°C). Here neither the sympathetic nucleation process nor the uniform nucleation process appear operative. Instead, a thick α layer forms along grain boundaries with smaller numbers of α precipitates forming randomly in the grain interior (Figure 10). This reduced number of internal α-precipitates reflects the lower driving force for α nucleation as T_a approaches the β-transus.

Figure 11 is a schematic T-T-T diagram which summarizes these various precipitation regimes. It should be emphasized that this particular aging study is based strictly upon small β-ST specimens that have been quenched and isothermally aged. As primary α is introduced into this alloy, or as the β dislocation structure is altered by working, these curves will shift. At present we have not studied dislocation structure effects in a specific way, although by analogy to other β alloys we would expect high dislocation densities to accelerate α- phase formation markedly.[14] Our limited work with primary α bearing material indicates that only minor repositioning of these curves takes place as α_p content is altered. The curves are also highly dependent on rate of heating to T_a. For example, β-ST specimens aged in an air furnace at 500°C for one hour showed only non-descript uniform precipitation. Presumably this was due to slower specimen heat-up, and an increased time in the uniform α region of Figure 11. As indicated in this figure, continued aging in the higher temperature regime does not cause the fine uniform α to be replaced by sympathetic plates.

D. Stress Assisted Transformation

As mentioned earlier, 10-2-3 is sufficiently stabilized to prevent the formation of athermal martensite product upon quenching. As in other Ti systems,

- 12 -

however, the application of a relatively small external stress to the solution treated and quenched structure leads to the formation of martensite. In 10-2-3, X-ray diffraction has shown that the martensitic product has the orthorhombic structure characteristic of α''.[15] This α'' structure has atoms positioned at (0,0,0), (a/2, b/2, 0), (0, 2b/3, c/2), (a/2, b/6, c/2). Specifically, the lattice parameters are:

$$a = 3.01\text{Å}$$
$$b = 4.83\text{Å}$$
$$c = 4.62\text{Å}$$

Examples of the stress induced α'' phase are shown in Figure 12. Note in Figure 12a that α'' plates seldom terminate within a grain. Instead, the plates propagate through the β grain until either a grain boundary or another plate is encountered. The "wavy" appearance of α'' in some grains shown in Figure 11a demonstrates that α'' plate growth is deflected by subgrain boundaries, but that these obstacles do not stop plate propagation.

A small amount of mechanical twinning of the {112} <111> type has also been observed by TEM in 10-2-3. These plates are optically indistinguishable from α'' and thus no attempt has been made to determine the relative volume fractions of α'' and twinned β.

II. Mechanical Behavior

The effects of the aforementioned microstructural variations on simple stress-strain relations during tensile testing have been briefly examined. Some of the more important results are summarized in Table I, and are discussed below.

A. Solution Annealed Conditions (Unaged)

Both the β-ST and the $\alpha+\beta$-ST conditions of 10-2-3, shown in Figures 2a and 2b, are microstructurally simple. Nevertheless, they possess some very interesting tensile characteristics. One important characteristic of this alloy

(and other Ti alloys) is the effect of α_ρ volume fraction on Young's modulus, E. Unlike most systems, E does not vary according to the rule of mixtures when α is introduced to a β matrix. This results from solute partitioning to the β-phase as the volume fraction of α_ρ is increased, which concurrently increases the modulus of β. Thus, the modulus of the two phase alloy can be estimated only if the actual β-phase modulus is used in the calculation.

When discussing strength levels of various $\beta+\alpha_\rho$ unaged structures, one should consider the relative importance of three contributions:

> 1) Second phase strengthening by the α_ρ dispersion.
>
> 2) Solid solution strengthening of the β matrix by solute enrichment.
>
> 3) The relation between mechanical stability of the β-phase, and the β composition.

Due to the large α_ρ spacing and to the large plastic strains associated with α'' formation, only the latter of the three is important when discussing the mechanical behavior of ST 10-2-3.

Beta is far more unstable in quenched β-ST 10-2-3 than in quenched $\beta+30\%$ α-ST. Consequently β-ST material is far more susceptible to the stress-induced transformation discussed above. Figure 13 compares yield stress, UTS, and elongation to failure for three levels of β stability. Note that while the UTS values are experimentally identical, the yield stresses are drastically different. The stress-strain curves illustrate this effect. In β-ST material, the β-α'' transformation initiates the onset of plastic strain at stresses as low as 250MPa. The driving force for α'' nucleation is provided by the elastic strain energy of the β matrix. The first plates to nucleate are free to extend the full length of the β grain, and may, in fact, provide

- 14 -

nucleation sites in an adjacent grain (Figure 12). The large increase in martensitic volume fraction per plate and the resulting large plastic strain increment associated with each nucleation event accounts for the apparent "easy glide" region directly following yield. Plates nucleated at a later time are mechanically stopped because the parent β-phase has been partitioned by previously transformed plates. These plates produce a smaller plastic strain. Partitioning of the β-phase may also increase the stress needed to nucleate new plates. Thus, an inflection point is observed in the σ-ε curves, followed by a rapid rise in σ (ε). This rapid rise may also be partly due to second phase strengthening by the α" plates. The result of this rapid strain hardening is an extended plastic region prior to failure.

The effect of inclusions on mechanical behavior of 10-2-3 was only qualitatively investigated since no inclusion free material was available for comparison. Figure 14a shows the tensile fracture surface of a β-ST specimen. The dimple size correlates very well with the inclusion spacing and, in fact, an inclusion can be found in virtually every dimple. Figure 14b shows the fracture surface of an α-β ST specimen (30% α_ρ). Here the one-to-one dimple-inclusion correlation is poorer and instead the dimples appear to correlate more closely to the α_ρ dispersion. From this we conclude that in the absence of coarse α particles, inclusions may act as crack nucleation sites, but that when α_ρ is present, it also plays a role in void nucleation.

The athermal ω found in the ST and quenched conditions does not seem to have any great effect on mechanical response, but since this condition cannot be tested without ω_a, such effects cannot be accurately determined.

B. β-Solution Treated and Aged Conditions

Specimens with low volume fractions of ω were characterized by very low

work hardening rates and uniform ductilities. Specimens with higher ω volume fractions were brittle, and fractured without macroscopically yielding. Specimens aged for 12hr at 300°C and tested in compression were also completely brittle and shattered during testing. There have been attempts in the past to understand the brittle nature of β alloys containing the ω-phase.[16-18] We agree that this type of behavior can only result from particle shearing. Shearing acts to destroy the ω particles and results in localized reductions in flow stress and in high dislocation concentrations in narrow slip bands. The resulting pile-ups at grain boundaries may result in stress concentrations, void nucleation, and rapid premature fracture.

All β-ST specimens aged in the uniform α regime of Figure 11 also were brittle. The strength levels of these fine precipitate dispersions are expected to be very high. The nature of this brittle mechanism is unclear, but work is currently underway to better understand this phenomenon. Transition region specimens are also quite brittle. For example, at 400°C, specimens aged for 10, 100, and 1000 minutes all failed prior to yield. It should be noted, however, that all specimens containing fine uniform α are not necessarily brittle, only that aged β-ST specimens containing fine α are brittle. β-ST specimens that lie entirely in the plate α regime have reasonable ductilities coupled with high strengths. As shown in Table I, yield stresses of 180 ksi with 9% elongation to failure are obtainable.

C. α+β Solution Treated and Aged Conditions

All aging treatments discussed above were preceded by a β-ST. Commercially, it is more useful to study the aging response in α+β ST specimens. Although the small amounts of α_ρ present after commercial α+β ST do not seem to affect the basic microstructural findings above, there are important effects of α_ρ on the

mechanical response of aged 10-2-3.

As we discussed earlier, during α+β solution treating, the ST temperature selection controls β matrix composition as well as the volume fraction of α_p. The β matrix composition also controls the volume fraction of α-phase which can be precipitated during aging. Thus, as the ST temperature increases, strength also increases. Conversely, ductility can be improved at the expense of strength by decreasing the ST temperature. Thus, the brittleness of the above mentioned uniform α regime can be avoided. By reducing the ST temperature to 720°C, and equilibrating about 25 volume percent α_p, it is possible to achieve yield strengths of 180 ksi with ductilities of 9% and UTS values of 225 ksi. Work is now underway to further examine the relationship of α_p to ductility and strength.

SUMMARY

Detailed microstructural work has revealed a number of transformations and transformation products which may occur in Ti-10-2-3.

1. <u>Athermal omega</u> appears upon rapid quenching of ST material. Although these fine non-descript particles have no discernible effect on mechanical properties, they affect subsequent aging behavior by catalyzing isothermal ω-phase and/or α-phase formations.

2. <u>Isothermal omega</u> is discussed as the continued displacive-growth of athermal omega. Three morphologies of omega are shown: non-descript, ellipsoidal, and cuboidal. A rationale for these morphelogies is presented. Microstructures containing isothermal omega are generally characterized by low work hardening rates and low ductilities.

3. <u>Uniform alpha</u> of both the Burger's and non-Burger's variety was found at low aging temperatures (below 400°C). This type of α appears to nucleate on particles of isothermal omega. With continued aging this α changes from a blocky morphology into fine "stubby" plates uniformly distributed throughout the β matrix. The fine nature of these dispersions allow very high strengths to be achieved, even in ST specimens containing as much as 25% α_p.

4. <u>Sympathetic plate alpha</u> of both the Burger's and non-Burger's type was observed above 400°C. These precipitates were shown as large plates of very high aspect ratio. The sympathetic nature of precipitation was demonstrated by examining the competition of this mechanism with the uniform mechanism of above. Although these coarser plates do not strength as efficiently as the fine uniform dispersions, very high strengths are nonetheless achievable in β-ST material.

5. <u>Grain boundary alpha</u> is present above 400°C, but appears in increasing thickness as the aging temperature is increased. The propensity for α formation at grain boundaries relative to the grain interiors increases as aging temperatures are increased.

6. <u>Orthorhombic martensite (α'')</u> is found only in stressed 10-2-3. The transformation can be inhibited by the precipitation of α, and the associated chemical stabilization of β. The formation of α'' decreases yield stresses by plastically accommodating relatively small elastic strains.

In addition to the above transformations, inclusions were found. Analytical STEM techniques showed these inclusions to be rich in Ti, P, S, and Si. Chemical banding, which is found in many other β alloys, was demonstrated to be due to iron segregation.

ACKNOWLEDGMENTS

REFERENCES

1. C. Chen, unpublished research.

2. J. A. Hall, unpublished research.

3. C. Chen and R. R. Boyer, Jl. of Metals, 31, 33 (1979).

4. Y. A. Bagaryatski, T. V. Tagvnova, and G. I. Nosova, Dokl. Akad. Nauk SSSR, 105, 1225 (1955).

5. D. de Fontaine, N.E. Paton, and J. C. Williams, Acta Met., 19, 1153 (1971).

6. H. E. Cook, Acta Met., 22, 239 (1974).

7. J. M. Silcock, Acta Met., 6, 481 (1958).

8. M. J. Blackburn and J. C. Williams, TMS-AIME, 242, 2461 (1968).

9. W. G. Brammer and C. G. Rhodes, Phil Mag., 16, 477 (1967).

10. B. S. Hickman, Jl. Matls. Science, 4, 554 (1969).

11. J. C. Williams and M. J. Blackburn, TMS-AIME, 245, 2352 (1969).

12. C. G. Rhodes and J. C. Williams, Met. Trans., 6A, 2103 (1975).

13. H. I. Aaronson, Decomposition of Austenite by Diffusional Processes, V. F. Zackey and H. I. Aaronson, Eds., Interscience, NY, p 481, 1962.

14. c.f. L. A. Rosales and A. W. Sommer, N. A. Rockwell Technical Report NA-73-191.

15. c.f. J. C. Williams; Titanium Science and Technology, Vol. 3, R. Jaffee and H. M. Burte, Eds., Plenum Press, NY, p 1433, 1973.

16. J. C. Williams, B. S. Hickman, and H. L. Marcus, Met. Trans., 2, 1913 (1971).

17. A. Gysler, G. Lütjering, and V. Gerold, Acta Met., 22, 901 (1974).

18. R. G. Baggerly and J. C. Williams, unpublished research, Rockwell International, 1974.

TABLE I

Microstructure	Heat Treatment	σ_{ys}(MPa)	UTS (MPa)	e_u(%)	e_f(%)	RA(%)
20% α_ρ+β +ω_{ath}	730°C (48hr) +WQ	741	862	9.7	18.6	35.
β+ω_{ath}	850°C (2hr) +WQ	262	878	15.7	21.8	32.
α+β +ω_{iso}	700°C (300m) +WQ +250°C (6000m)	1218	1266	.26	.58	2.25
β+ω_{iso}	850°C (2hr) +WQ +250°C (10^4m)	Brittle-no yield	-	0	0	0
20% α_ρ +β+α (uniform)	720°C (100m) +WQ +370°C (1000m)	1240	1430	2.7	8.9	16.
β+ α (uniform)	850°C (100m) +WQ +370°C (1000m)	Brittle-no yield	-	0	0	0
20% α_ρ +β+α(sympathetic)	730°C (12hr) +WQ +500°C (60m)	1063	1106	4.6	17.5	58.
β+ α (sympathetic)	850°C (100m) +WQ +500°C (240m)	1225	1243	2.3	8.7	14.
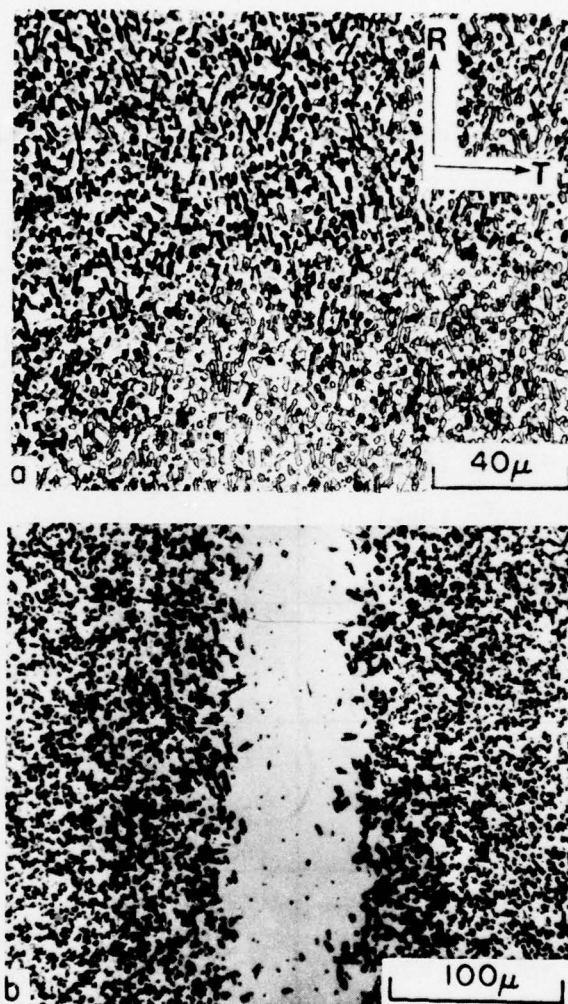
Figure 1 - Optical micrographs of Ti-10V-2Fe-3Al (a) as hot rolled and prior to aging, and (b) as solution treated in the α+β field to emphasize chemical banding. The rolling direction (R) and the short transverse direction (T) are shown. Part (b) is oriented the same way.
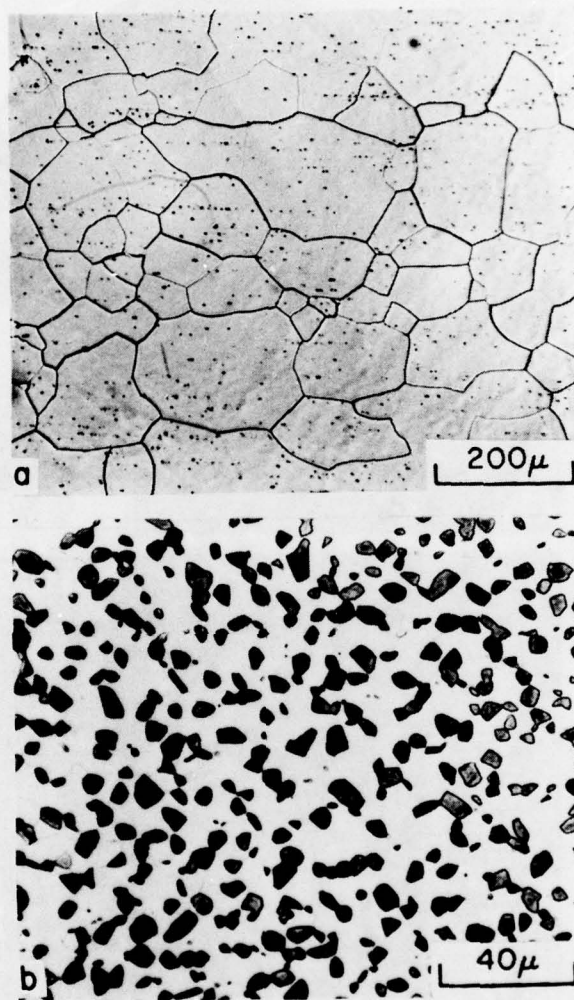
Figure 2 - Optical micrographs of solution treated Ti-10-2-3:

(a) β-ST (850°C - 15 m), and

(b) α+β-ST (730°C - 10,000m).
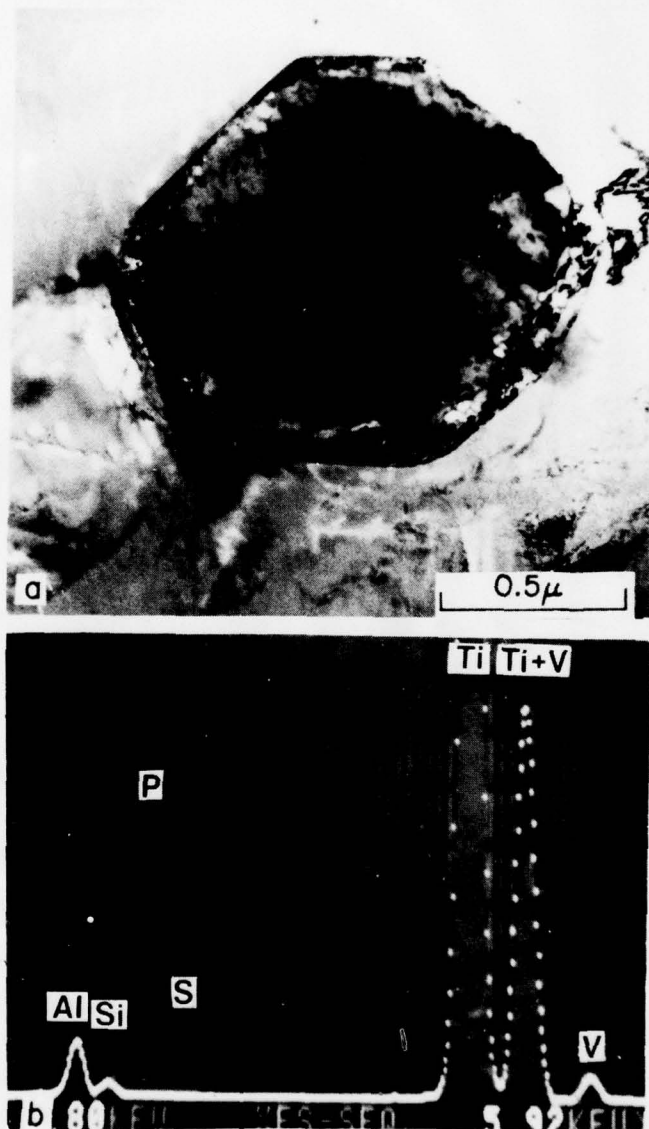
Figure 3 - (a) Conventional TEM micrograph showing an inclusion in 10-2-3, and

(b) the energy dispersive X-ray spectra from the inclusion and

the adjacent matrix. Matrix spectrum is shown in outline, inclusion

spectrum in solid.

24
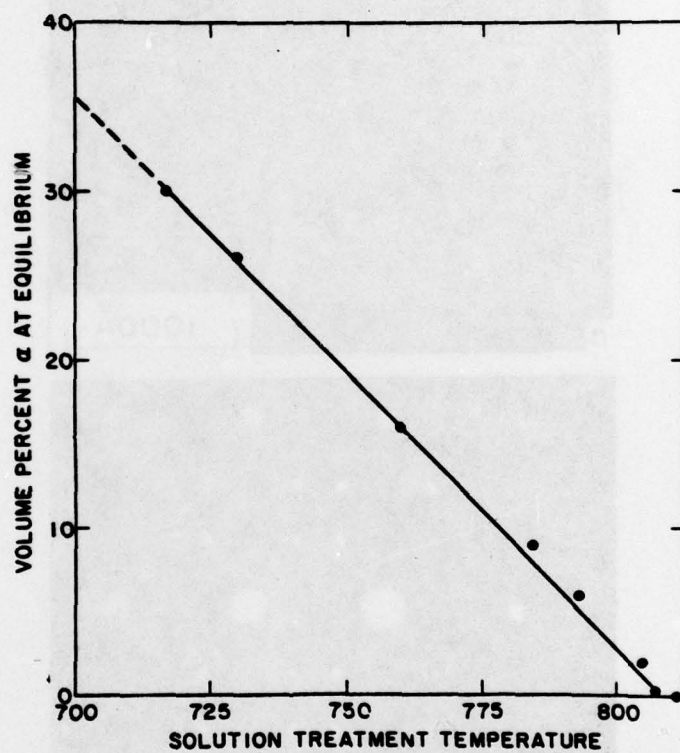
Figure 4 - Plot illustrating the dependence of equilibrium α content on ST temperature.

Figure 5 - Athermal ω (ω_{ath}) shown in the β-ST condition: (a) TEM dark field, and (b) [110] β-zone electron diffraction pattern.
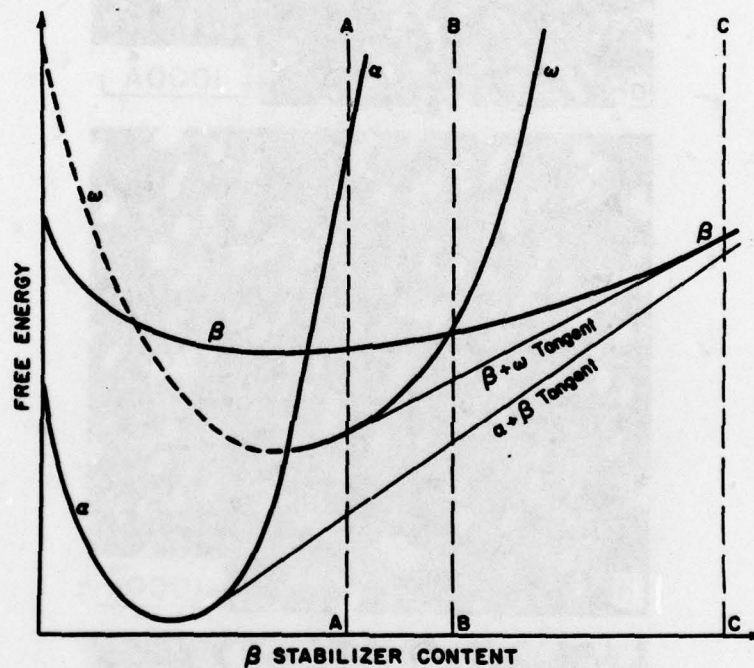
Figure 6 - A schematic representation of the α, β, and ω free energy curves
for a hypothetical binary β-stabilized Ti system at an arbitrary
temperature.
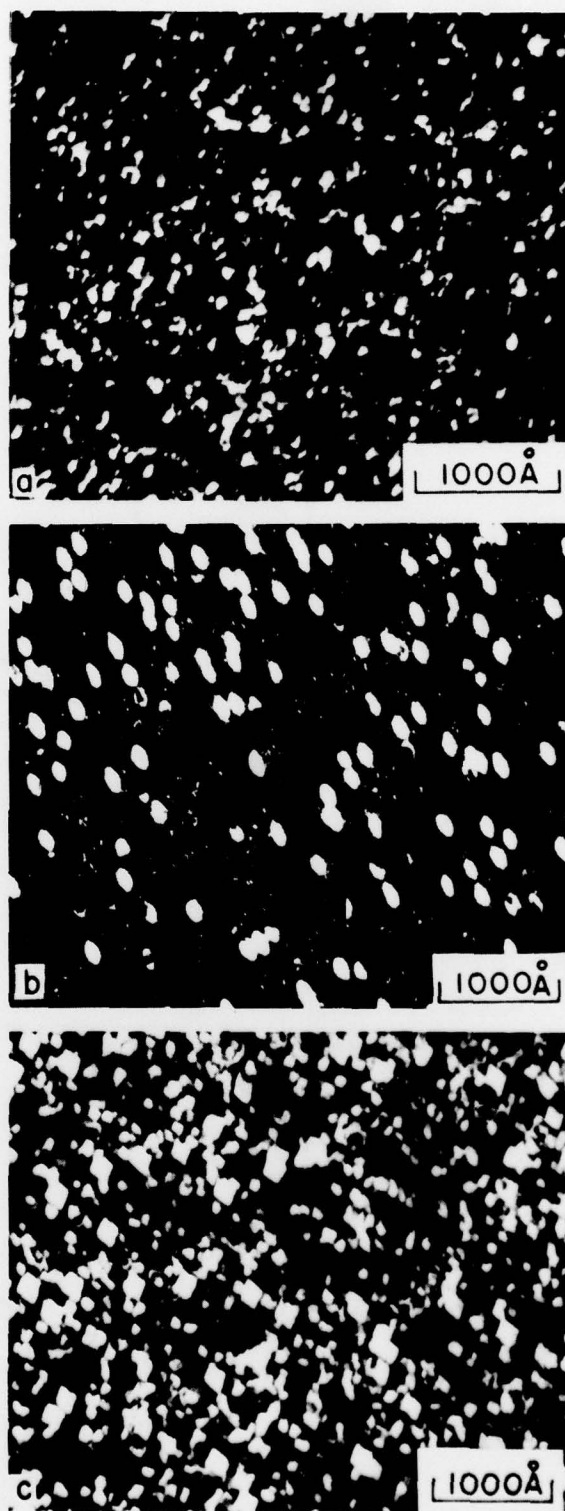
Figure 7 - Dark field TEM micrographs illustrating the three omega morphologies found in β-ST and aged Ti-10-2-3: (a) non-descript (250°C - 10,000m), (b) ellipsoidal (400°C - 1m), and (c) cuboidal (400°C-1m + 300°C-45m).

28
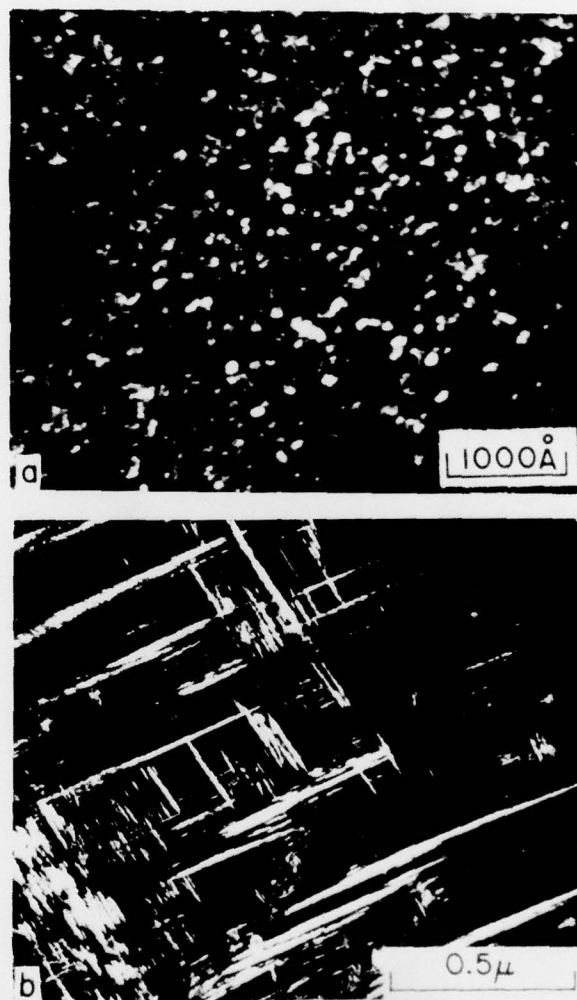
Figure 8 - Dark field TEM micrographs of the two α morphologies found in Ti-10-2-3 aged at 400^OC for 10 m.

(a) fine uniform α, which will quickly develop a "stubby" plate morphology, (b) sympathetically grown, non-uniform plates with very high aspect ratios.
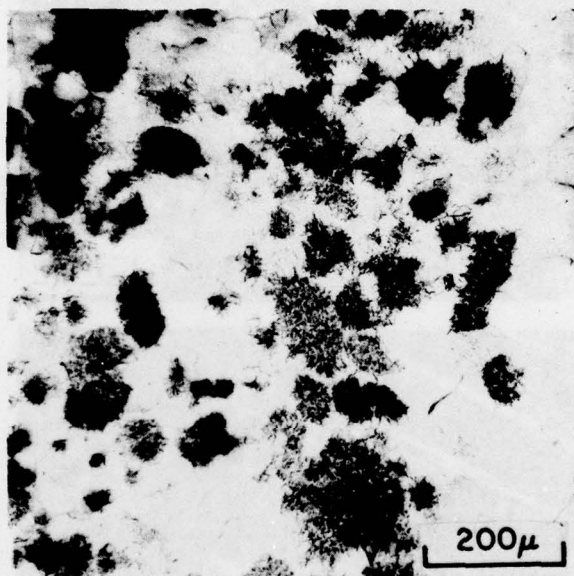
Figure 9 - Optical micrograph showing both types of α after 100 m at 400°C;
the darkly etched regions contain sympathetic α, while the
apparently clear unetched areas contain the uniform product.
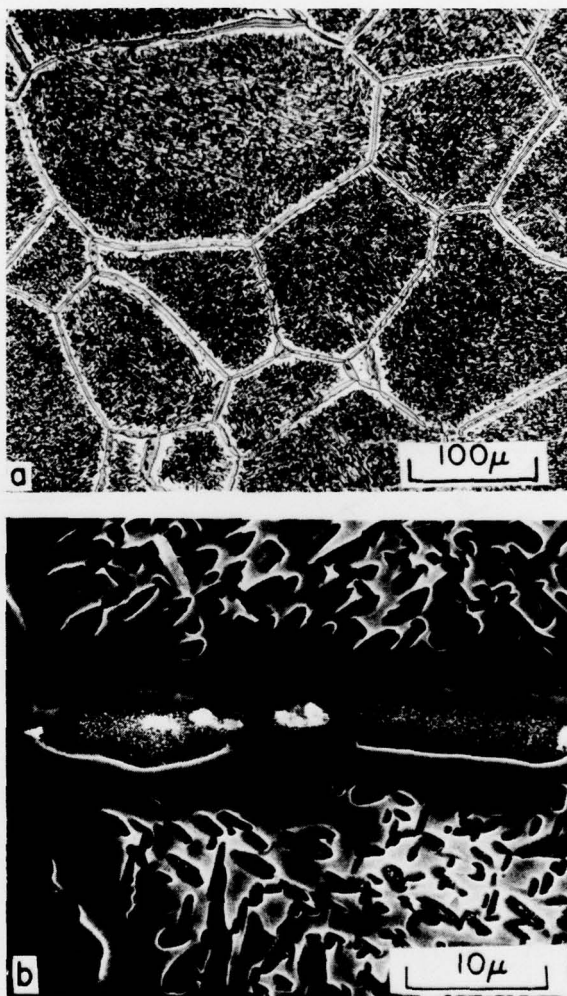
Figure 10 - Grain boundary α layers in β-ST + aged (680°C - 2000m) Ti-10-2-3: (a) optical micrograph, (b) SEM micrograph. Note inclusions collected along grain boundary.
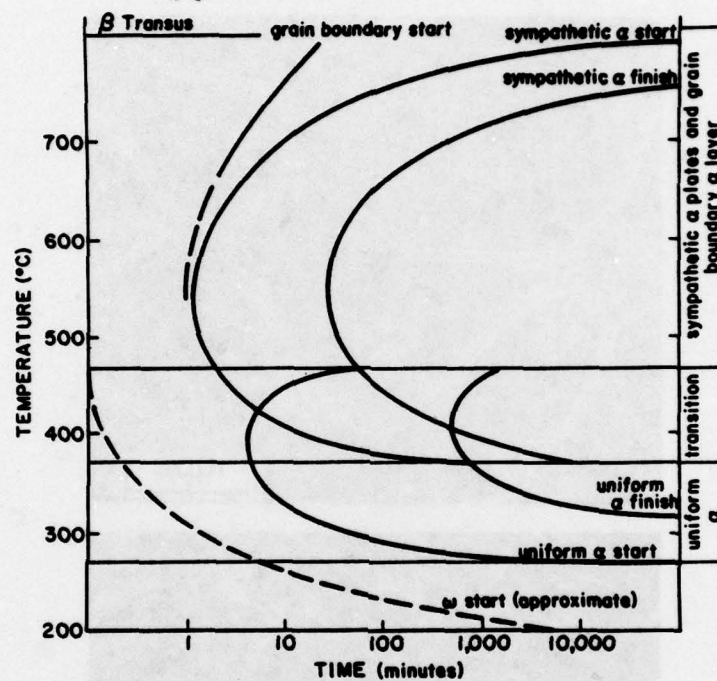
Figure 11 - Qualitative TTT diagram for β-ST Ti-10-2-3, illustrating the
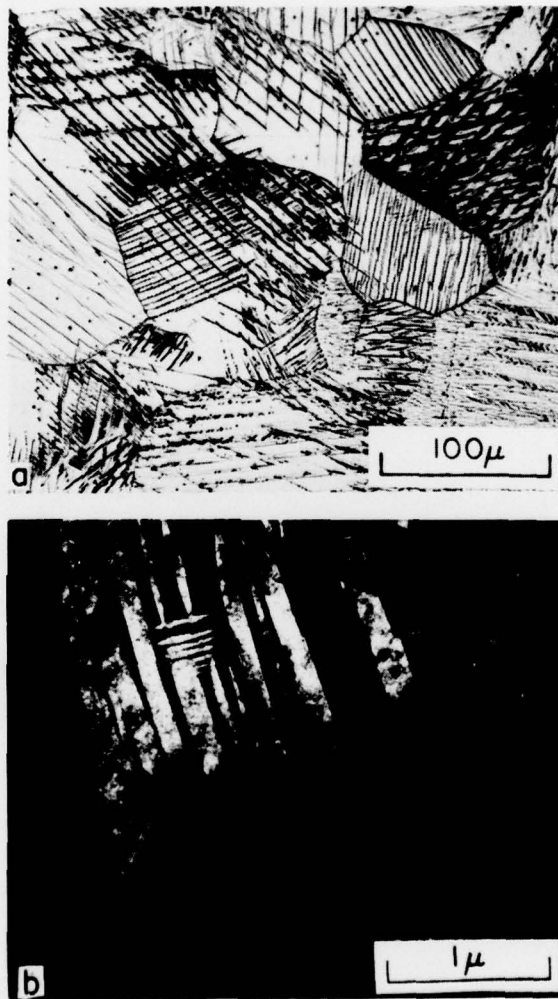
competition between nucleation regimes.

Figure 12 - Microstructures of deformed β-ST material.   (a) optical micrograph,

(b) TEM darkfield micrograph.
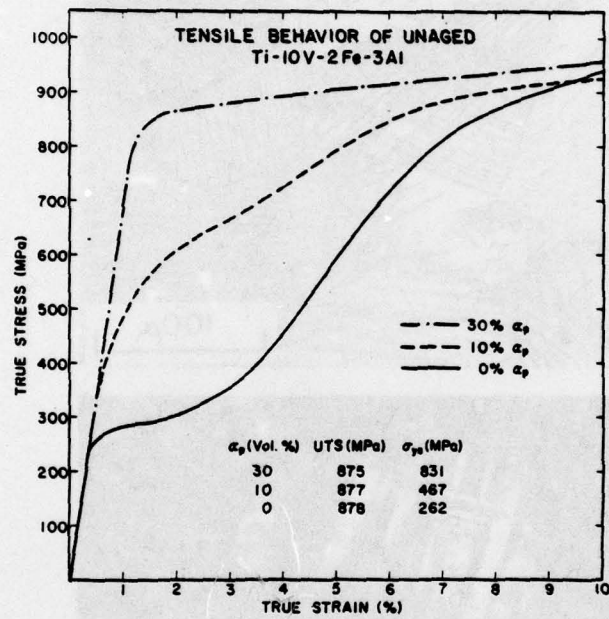
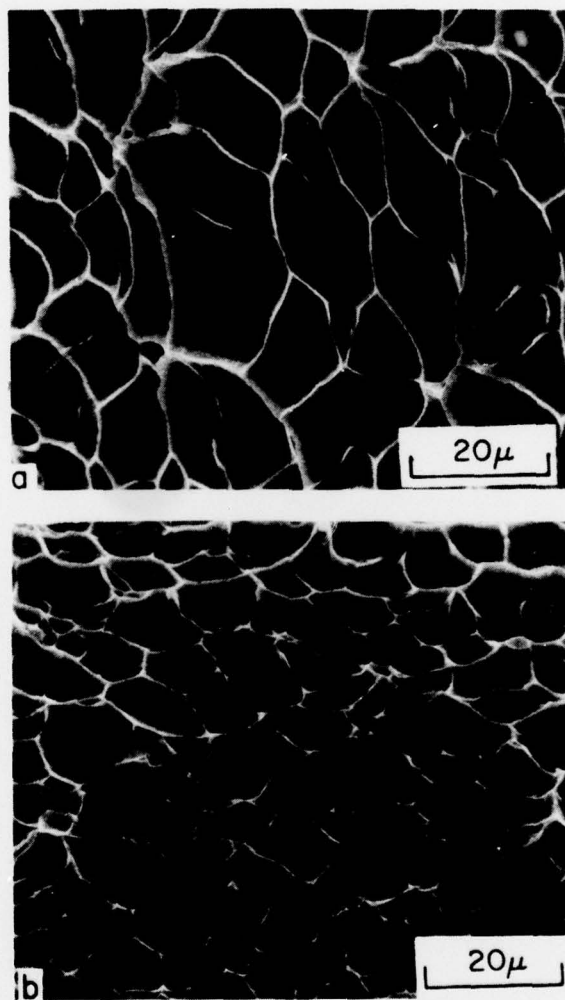Figure 13 - True stress-strain curves for three levels of β stability.

Figure 14 - SEM fractographs of unaged (a) β-ST tensile, and (b) α+β-ST (with ∿ 30% α_ρ) tensile specimens.

REPORT DOCUMENTATION PAGE

1. REPORT NUMBER	2. GOVT ACCESSION NO.	3. RECIPIENT'S CATALOG NUMBER
JWTR-5		

4. TITLE (and Subtitle)	5. TYPE OF REPORT & PERIOD COVERED
Phase Transformations and Tensile Properties of Ti-10V-2Fe-3Al	Technical Report.
	6. PERFORMING ORG. REPORT NUMBER

7. AUTHOR(s)	8. CONTRACT OR GRANT NUMBER(s)
T.W. Duerig, G.T. Terlinde and J.C. Williams	N00014-76-C-0409

9. PERFORMING ORGANIZATION NAME AND ADDRESS	10. PROGRAM ELEMENT, PROJECT, TASK AREA & WORK UNIT NUMBERS
Carnegie-Mellon University Pittsburgh, PA 15213	

11. CONTROLLING OFFICE NAME AND ADDRESS	12. REPORT DATE
Office of Naval Research 600 N. Quincy Arlington, VA 22217	August 1979
	13. NUMBER OF PAGES
	35

14. MONITORING AGENCY NAME & ADDRESS(if different from Controlling Office)	15. SECURITY CLASS. (of this report)
39p.	Unclassified
	15a. DECLASSIFICATION/DOWNGRADING SCHEDULE

16. DISTRIBUTION STATEMENT (of this Report)

Unlimited

17. DISTRIBUTION STATEMENT (of the abstract entered in Block 20, if different from Report)

Unlimited

18. SUPPLEMENTARY NOTES

Manuscript submitted for publication in Metallurgical Transactions

19. KEY WORDS (Continue on reverse side if necessary and identify by block number)

Ti-10V-2Fe-3Al, Ti Alloys, Nucleation and Growth, Omega Phase, Stress Induced Transformations, Inclusions

20. ABSTRACT (Continue on reverse side if necessary and identify by block number)

The effect of heat treatment on the microstructure of the metastable beta alloy Ti-10V-2Fe-3Al has been studied using light and electron metallography, analytical electron microscopy, and X-ray diffraction. A limited survey of the effect of microstructure on tensile properties of the alloy also has been conducted. It has been found that the alloy contains inclusions which are rich in Ti, S, Si, and P. The alloy has been shown to form the omega phase both athermally and isothermally. The isothermal omega can have either an

ellipsoidal or a cuboidal morphology. The reasons for this are enumerated The formation of the equilibrium alpha phase has been studied, and three distinct modes of formation are described. A stress induced othorhombic martensite also has been observed. The effect of theis stress induced product on tensile behavior is discussed. The relative roles of inclusions and alpha phase precipitates on tensile fracture also have been examined.